# Low-Frequency Power-Grid Ancillary Services From Commercial Building HVAC Systems

Yashen Lin*, Prabir Barooah*, and Sean P. Meyn†

*Department of Mechenical Engineering, University of Florida
†Department of Electrical and Computer Engineering, University of Florida

***Abstract*—With the introduction of volatile renewable energy sources into the grid, the need for inexpensive ancillary service increases. We propose a method to provide ancillary service by using the flexibility of demand in commercial building HVAC (Heating, Ventilation, Air-Conditioning) systems. In particular, we show how a regulation command transmitted by a balancing authority can be tracked by varying the cooling demand in commercial buildings in real-time. A key idea here is the bandwidth limitation of the regulation signal, which allows the building's HVAC system to provide this service with little effect on the indoor climate. The proposed control scheme can be applied on any building with a VAV (Variable Air Volume) system and on-site chiller(s). Simple calculations show that the commercial buildings in the U.S. can provide 47 GW of regulation reserves in the frequency band $f \in [1/(60\,\text{min}), 1/(3\,\text{min})]$ with virtually no change in the indoor climate, while meeting current ISO/RTO standards for regulation.**

## I. Introduction

To ensure the functionality and reliability of a power grid, supply and demand must be balanced at all time-scales. Correcting the mismatch between them, which occurs due to many sources of uncertainty, requires ancillary service. A large amount of ancillary service will be required in the future if a large fraction of our energy needs is to be met from renewable energy sources with their associated unpredictability and volatility.

Traditionally, ancillary service to balance demand and supply in fast time-scales is provided through the supply side, via fast ramping generation. We argue that the demand side can supply the same balancing service, without significantly impacting the needs of consumers. Ancillary service from loads can be as reliable as that obtained through generation, and may be far less expensive in the long-run. Recent research has shown that thermostatic loads in particular, can provide ancillary service with the help of appropriate control algorithms; see [1], [2], [3] and references therein. These works focus on residential loads such as A/C and refrigerators.

Commercial buildings have a number of advantages over residential buildings in providing ancillary service by exploiting load flexibility. About 30% of all commercial building floorspace in the U.S. is serviced by VAV systems in which the air flow rate can be varied continuously between a low and high value [4]. This makes them particularly well-suited for sophisticated control. Moreover, many buildings are equipped with BAS (Building Automation Systems), making the task of implementing additional control algorithms easy and inexpensive. Finally, commercial buildings have high thermal inertia, which can be translated to effective energy storage much like a very large battery.

As illustrated in Fig. 1, different resources can provide ancillary service in different frequency ranges. Water pumping and coal generation are useful at the lowest frequencies, while gas-turbine generation, batteries, and the HVAC system of [8] provide ancillary service in higher frequency bands. Commercial buildings have also been used for demand response programs (see for example [5], [6], [7]), which typically involve reduction of peak power in emergency situations, which is far from the goal of the present paper.

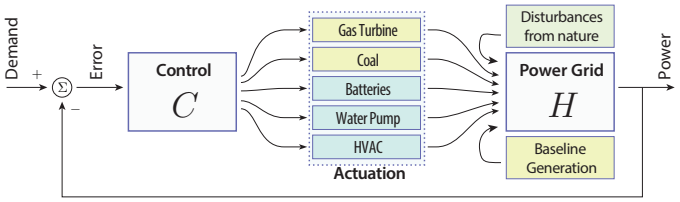


Fig. 1. Ancillary services interpreted as actuation in a control system.

The present work is a sequel to [8], in which control architectures are proposed for commercial building HVAC systems for providing ancillary services. A key observation is that reliable climate control and reliable ancillary service can be obtained, subject to constraints on the *magnitude* and *frequency bandwidth* of the ancillary service provided. It was shown that the fans in commercial buildings that have VAV HVAC systems in the U.S. can provide 70% of the regulation reserves in the frequency range $f \in [1/(3\text{ min})\ ,\ 1/(8\text{ sec})]$ (Hz).

In this paper, we extend the time-scale of ancillary service from commercial building HVAC system to the range 3 minutes to an hour by using the flexibility in the power demand from chillers. While [8] considers fans as the only source of flexible demand in commercial buildings, chillers are a much larger consumer of electricity, and hence a source of much greater ancillary service.

A key requirement is that indoor climate quality is maintained. This puts a limitation on the frequency band at which ancillary service can be provided. Low frequency deviations in airflow could result in significant temperature variations, depending upon the existing climate controller in the particular building. Typical climate controllers are designed to reject low-frequency temperature deviations. Consequently, low frequency power deviations may instigate the climate controller to reject resulting temperature deviations. The climate quality will be maintained, but the ancillary service will degrade due to the climate control power consumption. This ambiguity is resolved if the variation in the regulation reference has zero

978-1-4799-1526-2/13/$31.00 ©2013 IEEE

mean, and sufficiently high frequency.

Frequency and magnitude constraints are obtained by passing the regulation signal through a bandpass filter. Simulations with a calibrated dynamic model of a building HVAC system demonstrate that the frequency range $\mathscr{F}$ in which the proposed controller can provide ancillary service is $\mathscr{F} \triangleq [f_1,\ f_2]$, where $f_2 \leq 1/(3\,\text{min})$ and $f_1 \geq 1/(60\,\text{min})$. This range crosses both secondary control (1-10 min) and tertiary control (10 min - hours) [9].

There are a few challenges in designing control algorithms for harnessing ancillary service from commercial building HVAC systems in the time scales of interest in this paper. The first challenge is that the relevant dynamics of the cooling coil and air flow are complex. Tashtoush et al. [10] and Huang et al. [11] each propose a model for a VAV HVAC system. However, there are large number of parameters that are hard to obtain accurately. Given that we are interested in regulation in a restricted frequency range, a simpler model for control is proposed. The model is calibrated and validated with field data collected from Pugh Hall in the University of Florida campus.

The second challenge is that there is a transport delay between the change in air flow and the change in power consumption in the chiller, due to the time required for the chilled water to flow from the cooling coil back to the chiller. Reference tracking despite the time delay is achieved by a combination of a Kalman predictor and a Smith Predictor: the Kalman predictor is used to predict the future reference and the Smith predictor is used to ensure closed loop stability in presence of delay. The controller is designed on a linearized version of the plant, which is a hybrid-nonlinear system.

Simulations show that the proposed control architecture provides high-quality ancillary service, according to the criteria established by PJM [12], while having little impact on indoor climate. Parametric variation studies show that the controller is also robust to potential mismatch between the true value of the transport delay and that used in the design.

The rest of the paper is organized as follows. The overall control architecture is presented in Sec. II. For the purpose of controller design, we need dynamic models of the components involved; which are described in Sec. III. Controller design is explained in Sec. IV. The performance of the controller is then tested through simulations on the original non-linear model of the system. Results are described in Sec. V.

## II. Proposed Control Architecture

A schematic of a typical single-zone VAV HVAC system used in a commercial building is shown in Fig. 2. Part of the return air is mixed with outdoor air and sent into the AHU (Air Handling Unit), where it is cooled and dehumidified by passing it across a cooling coil. The conditioned air is then supplied to the zone by a supply air fan. A control system maintains the discharge air temperature at a pre-specified set-point, usually $55^o$F, by varying the flow rate of chilled water passing through the cooling coil. The inlet temperature of the chilled water into the cooling coil is usually constant, at around $44^o$F. An indoor climate controller varies the rate of supply airflow to maintain the temperature of the space at a pre-determined set-point. The power consumption of the chiller is directly affected by variation in the airflow rate since conditioning more air requires more cooling energy.

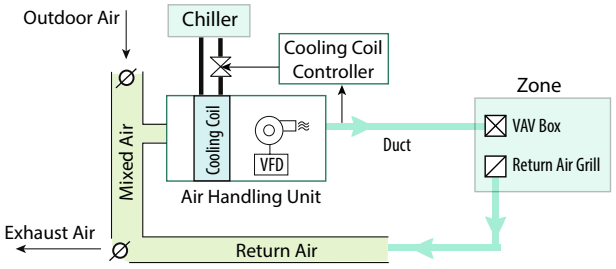


Fig. 2. Typical commercial building VAV HVAC system with a single zone.

Our objective is to vary the instantaneous power consumption in chiller and fan to provide ancillary service. In the proposed control architecture, a *regulation reference signal*, denoted by $\tilde{P}_r$, will be transmitted to each participating building. We take the ACE (Area Control Error), which indicates the imbalance in the grid [9], scale it down by a scaling factor and feed it through a bandpass filter to define $\tilde{P}_r$.

A local controller at a building - that we call *the regulation controller* - will manipulate the supply air flow rate in the building so that the deviation of the instantaneous power consumption from the baseline power tracks the regulation reference signal. "Baseline" value of a variable refers to the counterfactual: the value of the variable due to the actions of the closed loop control system that operates the HVAC system, in the absence of the regulation controller. The reasons for choosing the flow rate of air as the control command are that this variable has a large influence on the power consumption, and it can be easily commanded using the building automation system.

Fig. 3 shows a schematic representation of the signal flow in the proposed control architecture. It should be emphasized that the proposed architecture does not replace the existing building climate controller. It merely modifies the commanded rate of airflow.

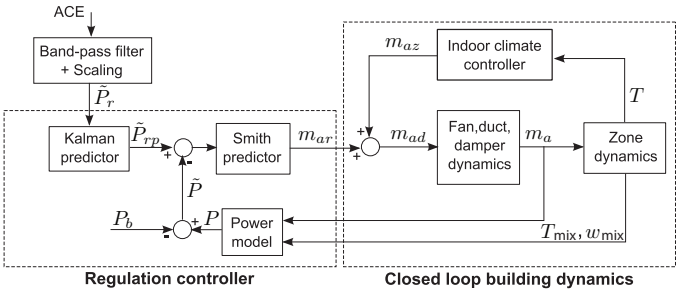


Fig. 3. Proposed control architecture.

The reference signal $\tilde{P}_r(t)$ is fed into a Kalman predictor to predict the future reference signal $\tilde{P}_{rp} = \hat{\tilde{P}}_r(t+t_d)$, where $t_d$ is the transport delay in the chiller power. More detail can be found in Sec. IV. Let $\tilde{P}(t) = P(t) - P_b(t)$ be the deviation of the measured power consumption from the baseline $P_b(t)$. The goal of our regulation controller is to compute the desired additional supply air flow rate $m_{ar}(t)$ which drives $\tilde{P}_{rp}(t) - \tilde{P}(t)$ to 0. The building's existing indoor climate controller

computes the desired supply air flow rate $m_{az}(t)$ based on zone temperature. The sum of $m_{ar}(t)$ and $m_{az}(t)$, denoted by $m_{ad}(t)$, is the desired supply flow rate, which is commanded though the BAS. The building's HVAC control system commands the fan and dampers to produce this air flow rate. The actual airflow flow rate $m_a(t)$ is the output of a closed loop control system that depends on the dynamics of the fan controller, damper, and airflow in ducts. Part of the exhaust air from the zone will be mixed with outdoor air in the AHU. The mixed air temperature $T_{mix}(t)$, humidity ratio $w_{mix}(t)$, and mass flow rate $m_a(t)$ determine power $P(t)$ consumed by the chiller and fan.

## III. Building HVAC system modeling

This section presents the dynamic model for each part of the HVAC system shown in Fig. 2. Parameter estimation will be discussed in section V-A.

### A. Zone thermal dynamics

Zone temperature and humidity are the two main state variables of interest. Temperature dynamics can be captured by a RC (resistor-capacitor) circuit analogy [13], [14]. In this paper, we adopt the 2*R*-2*C* model suggested in [13], which is a second order nonlinear system. Dynamics of the zone humidity ratio is one of mass transfer, and is governed by a first order differential equation [14]. The zone thermal dynamics model has 3 states, 8 inputs, and 4 outputs. We omit more model details; they can be found in [15].

### B. Indoor climate controller and airflow dynamics

The so-called *single-maximum logic* is commonly used in commercial buildings to command the airflow so as to maintain the indoor temperature at a pre-determined set point and ensure adequate ventilation. It is a hybrid control logic that includes if-else conditions that determines control "modes" (i.e., when to blow cold air and when to reheat), along with proportional controllers that determine the amount of airflow in each mode. Due to lack of space, we refer the interested reader to [16], [17] for details.

Once the climate controller computes the desired supply air flow rate, it is transmitted to the fan controller. The fan controller varies the fan speed to deliver the desired air flow rate. We model the closed loop system from the desired supply air flow rate $m_a^{ref}$ (input) to actual supply air flow rate $m_a$ (output) to be a first order system,

$$m_a(s) = \frac{1/\tau_f}{s+1/\tau_f} m_a^{ref}(s) \tag{1}$$

where $\tau_f$ is the time constant of the system. This time constant aggregates the dynamical effect of the inertia of the fan and dynamics of airflow through ducts.

### C. Cooling coil dynamics

Heat and moisture are removed from air at the cooling coil at the AHU. The dynamics of a cooling and dehumidifying coil are complex with many unknown parameters [18], [19]. In this paper, we adopt the idea of adding a time constant to a steady state model – as done in [20] – to get a first order dynamical model for the cooling coil. We use the subscript $a$ for air side, $w$ for water side, 1 for inlet conditions, and 2 for outlet conditions. The inlet and outlet water mass flow rate are the same, i.e., $m_{w1} = m_{w2} = m_w$. The inlet and outlet air mass flow rates are also assumed to be equal since the difference due to water vapor condensation is small, i.e., $m_{a1} = m_{a2} = m_a$. The inputs of the cooling coil are the inlet air and water conditions: $u_{cc} = [T_{a1}, w_{a1}, m_a, T_{w1}, m_w]^T$, outputs are the outlet air and water conditions: $y_{cc} = [T_{a2}, w_{a2}, T_{w2}]^T$.

Suppose the steady state input-output relations are given by $y_{cc} = g(u_{cc})$, $g : \mathbb{R}^5 \to \mathbb{R}^3$, which is determined by the design parameters of the cooling coil. We then linearize it around the design conditions, which are denoted by $u_{cc}^*$ and $y_{cc}^*$. By defining $\tilde{u}_{cc} = u_{cc} - u_{cc}^*$ and $\tilde{y}_{cc} = y_{cc} - y_{cc}^*$, we get

$$\tilde{y}_{cc} \approx J\tilde{u}_{cc},\ J = \frac{\partial g}{\partial u_{cc}}\,|_{u_{cc}^*} \tag{2}$$

Adding a single time constant to the steady state model (2), the cooling coil dynamics can be written as:

$$\tilde{y}_{cc}(s) = \frac{1/\tau_{cc}}{s+1/\tau_{cc}} J\tilde{u}_{cc}(s) \tag{3}$$

where $\tau_{cc}$ is the time constant of the open-loop cooling coil dynamics. Note that the Jacobian $J$ defines the DC gains of the transfer function from $\tilde{u}_{cc}$ to $\tilde{y}_{cc}$.

In practice, the cooling coil is under closed loop operation; see Fig. 2. The closed loop cooling coil model is obtained by using a PID controller which commands the chilled water flow rate to achieve desired conditioned air temperature. The closed loop cooling coil model is an LTI system with 2 states, 5 inputs and 3 outputs.

### D. Power consumption

The total power consumed $P(t)$ is the sum of fan power and chiller power: $P(t) = P_f(t) + P_c(t)$. The fan power is related to mass flow rate of air as $P_f = c_f m_a^3$, where $c_f$ is a constant coefficient which can be estimated from data [8].

The cooling and dehumidification of air occurs at the cooling coil, where the chilled water gains heat $Q(t)$ from the air: $Q(t) = m_w(t)C_{pw}(T_{w2}(t) - T_{w1}(t))$. The return water is cooled in the chiller where power is consumed. Due to the transport delay caused by the speed of water flow from the cooling coil to the chiller, which may be located far from the air handling unit, the power consumed by the chiller is

$$P_c(t) = \frac{1}{\eta_c} Q_c(t - t_d)$$

where $t_d$ is the delay and $\eta_c$ is the chiller efficiency.

## IV. Control design for ancillary service

The two major challenges in this regulation controller design are: (i) complex nonlinear hybrid dynamics of the HVAC system; (ii) transport delay in chiller power. We will linearize the system in design phase to tackle (i), and use a Smith predictor [21] and a Kalman predictor [22] to deal with (ii) so that the controller can be designed based on non-delayed system.

Consider the delay free case: $P_{nd}(t) = P_f(t) + Q_c(t)$. We combine dynamics of all the components of the HAVC system

with $m_{ad}$ as input, $P_{nd}$ as the output, with $x$ denoting the state vector and $w$ denoting the vector of external disturbances, which consists of inputs such as solar heat gain, internal heat gain, and ambient temperature. An equilibrium point $(x^*, m_{ad}^*, w^*)$ is chosen, where $m_{ad}^*$ is the nominal mass flow that is observed in normal operation and $w^*$ is the nominal value of all external signals including zone temperature set points, outside weather conditions, etc. The LTI approximation is then obtained by linearization around this equilibrium point:

$$\begin{aligned} \delta\dot{x} &= A\delta x + B\delta m_{ad} + E\delta w \\ \delta P_{nd} &= C\delta x + D\delta m_{ad} \end{aligned} \tag{4}$$

where $\delta x = x - x^*, \delta m_{ad} = m_{ad} - m_{ad}^*, \delta w = w - w^*, \delta P_{nd} = P_{nd} - P_{nd}^*$, and $P_{nd}^*$ is the equilibrium power consumption when $m_{ad}(t) \equiv m_{ad}^*, w(t) \equiv w^*$. The regulation controller is then designed as a compensator so that the closed loop sensitivity function $S(j\omega)$ is close to 0 in the frequency range of interest, and close to 1 otherwise, so that both reference tracking and disturbance rejection can be achieved.

To design a compensator to handle the transport delay discussed in Sec. III-D, we use a Smith predictor. The delay between mass flow rate change and chiller power consumption can be estimated from the flow rate of chilled water and the geometry and length of the pipe, which is used in the design of the Smith predictor. However, the Smith predictor does not achieve reference tracking. To be able to get reference tracking, we use a Kalman predictor to predict the reference signal $\hat{t}_d$ time units into the future, i.e., to obtain $\hat{\tilde{P}}_r(t+\hat{t}_d)$ where $\hat{t}_d$ is the estimated delay in the plant. The Smith predictor operates on the predicted reference so that the closed loop system is guaranteed to achieve reference tracking when $\hat{t}_d = t_d$.

The Kalman predictor uses a double integrator model of the process, with the first state being the reference signal, and the output being the reference signal corrupted by noise. The idea behind the model is that since the reference signal is smooth, it changes at an approximately constant rate in short time intervals. The continuous dynamics are first discretized, a standard Kalman predictor is then used to calculate the reference signal $n$ steps into the future [22]:

$$\hat{\tilde{P}}_r(k+n) = C_o A^n \hat{x}(k \mid k) \tag{5}$$

where $C_o = [1,0]$ is the output matrix, $\hat{x}(k \mid k)$ is the state estimated at time $k$ by the Kalman filter.

The accuracy of prediction depends on the bandwidth of the input and the delay. The reference signal $\tilde{P}_r$ is restricted to a frequency range $\mathscr{F}$ by bandpass filtering the ACE signal. The delay is estimated to be $30s$ for an on-site chiller in Pugh Hall. We ran the simulation with different delays, and it turns out the prediction error is reasonable up to 90s of delay. In reality, accurate knowledge of the delay may not be available. We study the effect of this uncertainty on prediction accuracy by performing simulations in which the true delay is $30s$ but the Kalman predictor uses a delay estimate of $20s$ and $40s$, respectively. The results are shown in Fig. 4, where the *error ratio* in the figure is defined as the ratio of prediction error to root mean square of the reference signal. The result shows that delay mismatch increases the prediction error, as expected, but not by a lot. Although the error appears to be large at some instances, it occurs when the magnitude of the reference signal is small. The effect of this error on reference tracking is further discussed in Sec. V-C, which shows that the resulting error in reference prediction is acceptable.

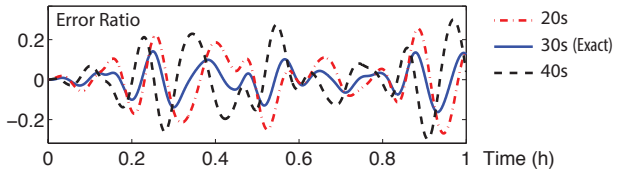


Fig. 4. Comparison of prediction errors of regulation reference signal $\tilde{P}_r$ when there is a mismatch between the true delay and delay used in the Kalman predictor.

## V. Simulation Study

### A. Simulation setup

The subsystems described in III are integrated together and implemented in *Simulink*. Field data was collected from Pugh Hall on University of Florida campus to estimate parameters in the model. We use data from AHU-2 in the building, which is used as a dedicated AHU for a large auditorium that is $22ft$. high with floor area $6000ft^2$, and can hold more than 200 occupants.

Zone parameters are estimated using the method in [13]. The measured zone temperature and the temperature predicted by the model are shown in Fig. 5 (left).

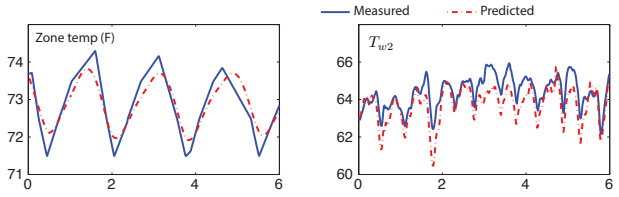


Fig. 5. Zone climate model (left) and cooling coil model (right) validation.

To estimate $J$ in the cooling coil model, we first pick a particular coil model that resembles the coil in AHU2 of Pugh Hall. For a given inlet conditions, the outlet conditions are obtained from *Daikin McQuay Tools Suite* [23]. The Jacobian is then estimated numerically. The outlet conditions predicted by the model and the measured outlet conditions are shown in Fig. 5 (right). Due to lack of space, only return chilled water temperature $T_{w2}$ is shown. It can be seen from the figure that our model predicts $T_{w2}$ well with a maximum prediction error less than $2^oF$.

Other parameter values are omitted due to lack of space; they are available in [15]. The baseline power $P_b$ is obtained by simulating the system without the frequency regulation controller. A profile of exogenous inputs, including ambient environment and solar and internal heat gain, are specified for the simulation. The values in the profile are chosen based on the location, construction, and schedule of Pugh Hall.

### B. Performance metrics

Performance of the control architecture depends on (i) how much ancillary service is provided through regulation reference

tracking, and (ii) how much deviation of the indoor climate from the baseline conditions occur as a result of the controller's actions.

Measuring regulation reference tracking is somewhat involved because of the way ancillary service is evaluated by ISOs. Traditionally, once certified, the frequency regulation service providers are usually compensated by capacity, not performance. However, this is unfair to those who provide faster or more accurate responses. FERC order No.755 [24] stressed this problem and asked RTOs and ISOs to design performance-based compensation in their tariff. In this paper, we will use the performance score defined by PJM [12].

The score contains three parts: $S_c$ - the correlation score, $S_d$ - the delay score, and $S_p$ - the precision score. $S_c$ and $S_d$ are used to quantify the delay between the regulation signal and the response of the resource. Define the correlation coefficient to be:

$$R_P(\tau) = \frac{cov(\tilde{P}_r(t), \tilde{P}(t+\tau))}{\sigma_{\tilde{P}_r(t)}\sigma_{\tilde{P}(t+\tau)}} \tag{6}$$

where $\sigma$ is the standard deviation of the signal. The parameter $\tau^*$ is defined as the time shift with which the response has the highest correlation with the reference signal:

$$\tau^* = \underset{\tau\in[0,5mins]}{\arg\max}\ R_P(\tau) \tag{7}$$

The scores $S_c$ and $S_d$ are then determined as:

$$S_c = R_P(\tau^*),\ S_d = \left|\frac{\tau^* - 5mins}{5mins}\right| \tag{8}$$

The precision score $S_p$ is defined as:

$$S_p = 1 - \frac{1}{n}\sum_{i=1}^{n}\frac{\left|\tilde{P}(i) - \tilde{P}_r(i)\right|}{\left|\tilde{P}_{r,a}\right|} \tag{9}$$

where $\tilde{P}_{r,a}$ is the hourly average of the reference signal, $n$ is the number of samples. The total performance score $S_t$ is the average of the three parts, i.e., $S_t = \frac{1}{3}S_c + \frac{1}{3}S_d + \frac{1}{3}S_p$.

### C. Results

ACE data from PJM is used as the regulation signal. The scaling factor need to be determined first. If the scaling factor is too large, the supply air flow rate has large oscillation, which is undesirable. First, it will violate the outdoor air requirement for indoor air quality when the supply flow rate becomes too low. Second, the oscillation increases wear and tear of the equipments. We evaluate the oscillation by comparing the variation from the baseline supply flow rate. More precisely,

$$v = \frac{1}{n}\sum_{i=1}^{n}\frac{\left|m_a(i) - m_{a,b}(i)\right|}{m_{a,b}(i)} \tag{10}$$

where $m_a$ is the supply flow rate with the regulation controller, $m_{a,b}$ it the supply air flow rate of the baseline case. We chose the scaling factor to be $4\times10^{-5}$, in which case $v = 15\%$.

The reference tracking results for two cases are shown in Fig. 6. The bandpass filter for the ACE signal is designed to have a passband of 3 to 30 minutes in case 1, and 3 to 60 minutes in case 2. From the figure, we see that in both cases

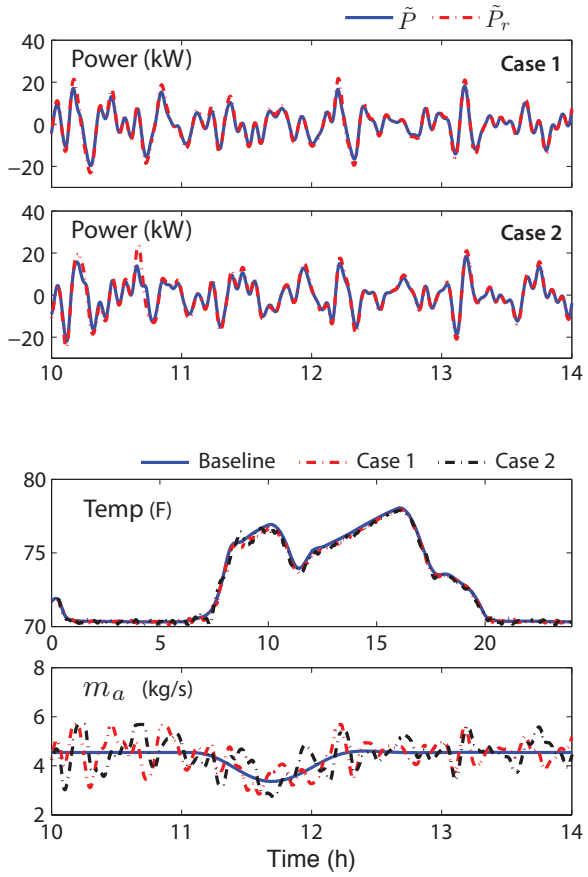


Fig. 6. Performance of the regulation controller

we are able to track the reference signal with maximum power of about $20KW$. The temperature deviation from baseline case is larger in Case 2 than in Case 1, but both are less than $1^oF$. The maximum temperature deviation $\Delta T_{max}$ $(^oF)$ and performance score $S_t$ are shown in Table I. The performance score is computed for each hour in a 12-hour duration, and then averaged. PJM require the provider to reach a score of 0.75 to be qualified for frequency regulation market. Our controller performs well above the requirement.

TABLE I. PERFORMANCE VS. REFERENCE FREQUENCY.

| Time scale (min) | $S_c$ | $S_d$ | $S_p$ | $S_t$ | $\Delta T_{max}$ $(^oF)$ |
|---|---|---|---|---|---|
| 1 to 3 | 0.67 | 0.85 | -0.95 | 0.50 | 0.24 |
| 3 to 10 | 0.96 | 1 | 0.82 | 0.93 | 0.10 |
| 10 to 30 | 0.96 | 1 | 0.81 | 0.92 | 0.44 |
| 30 to 60 | 0.95 | 0.95 | 0.80 | 0.90 | 1.69 |
| 3 to 30 (Case 1) | 0.96 | 1 | 0.81 | 0.92 | 0.40 |
| 3 to 60 (Case 2) | 0.96 | 0.98 | 0.79 | 0.91 | 0.87 |

We also tested the algorithm with reference signals of different frequency ranges by varying the passband $\mathscr{F}$ of the bandpass filter. The results are shown in Table I. The controller does not work well for high frequency range (1 to 3 minutes). Since the time constant of the chiller falls in that range, it cannot react fast enough to track the reference signal. The tracking performance of the middle and low frequency ranges are both good. However, the zone temperature variation from the baseline case grows as the reference signal becomes slower. That is because we are trying to over-condition or under-condition the zone for longer time periods, which drives the temperature away from the desired value.

The effect of chiller power delay mismatch on tracking performance was also studied in simulation. The true delay of the system is 30s. Table II shows the performance of the controller when it is designed assuming the delay is 15$s$ and 45$s$, respectively. As shown in the table, in both cases, the effect of chiller delay mismatch on the delay score $S_d$ is small. In the 45$s$ case, the precision score $S_p$ is worse compared to the case when accurate delay knowledge is used, but it is still acceptable. With this given model and reference signal, our control strategy is able to handle 50% of delay mismatch in both directions.

TABLE II. EFFECT OF DELAY MISMATCH IN CHILLER POWER.

| True Delay (s) | Delay in design (s) | $S_c$ | $S_d$ | $S_p$ | $S_t$ |
|---|---|---|---|---|---|
| 30 | 15 | 0.95 | 1 | 0.84 | 0.93 |
| 30 | 45 | 0.97 | 0.99 | 0.79 | 0.92 |

The simulation results show that AHU2 in Pugh Hall, which has a rated cooling capacity of 97.5 $KW$, could provide 20 $KW$ of ancillary service. The total regulation capacity of Pugh Hall ($46,000 ft^2$) that has two other AHUs is estimated to be 100 $KW$. In the U.S., the total floor area of commercial buildings is about $72,000$ million square feet, about 30% of which is served by VAV systems [4]. Assuming that the cooling power density ($KW$ per sq. ft.) is similar among these buildings, the commercial building sector could provide 47 $GW$ of regulation service, which is more than the total regulation capacity required in the U.S., which is about 10 $GW$ [25].

## VI. CONCLUSION AND FUTURE WORK

A large commercial building can be harnessed as a storage device because of its high thermal inertia. Consequently, HVAC systems can provide ancillary service, provided that the magnitude and bandwidth of regulation is constrained, so that climate quality is not significantly impacted.

Simulation results presented here shows the possibility of satisfying the entire regulation demand in the U.S. from commercial buildings. Compared to the work in [8], we are able to extend the bandwidth of regulation to $f \in [1/(60\text{ min}), 1/(3\text{ min})]$, and also increase the magnitude of ancillary service, by utilizing chillers in the HVAC system.

Estimation of the baseline power consumption on-line from measured data is an avenue of future work, which will be helpful to the implementation of the regulation controller. Other future work direction includes integrating reheat power and chiller dynamical model and dealing with larger transport delay.

There are many broader questions concerning the realization of the block diagram Fig. 1, where the goal is to minimize, at low cost, the use of carbon based fuels for actuation in real-time operations. We are considering other loads, such as pool pumps and data centers, and we are considering the impact of transmission and distributed information on reliability of the grid.

Research is supported by the NSF grants CPS-0931416 and CPS-1259040; the Department of Energy Awards DE-OE0000097 and DE-SC0003879; and US-Israel BSF Grant 2011506.

## REFERENCES

[1] D. S. Callaway, "Tapping the energy storage potential in electric loads to deliver load following and regulation, with application to wind energy," *Energy Conversion and Manage.*, vol. 50, no. 5, pp. 1389–1400, 2009.

[2] S. Koch, J. L. Mathieu, and D. S. Callaway, "Modeling and control of aggregated heterogeneous thermostatically controlled loads for ancillary services," in *Proc. PSCC*, 2011, pp. 1–7.

[3] J. L. Mathieu, "Modeling, analysis, and control of demand response resources," Ph.D. dissertation, University of California, Berkeley, 2012.

[4] "Commercial buildings energy consumption survey (CBECS): Overview of commercial buildings, 2003," Energy information administration, Department of Energy, U.S. Govt., Tech. Rep., December 2008. [Online]. Available: http://www.eia.doe.gov/emeu/cbecs/cbecs2003/overview1.html

[5] K. R. Keeney and J. E. Braun, "Application of building precooling to reduce peak cooling requirements," *ASHRAE transactions*, vol. 103, no. 1, pp. 463–469, 1997.

[6] P. Xu, P. Haves, M. A. Piette, & J. Braun, "Peak demand reduction from pre-cooling with zone temperature reset in an office building," 2004.

[7] S. Kiliccote, M. A. Piette, and D. Hansen, "Advanced controls and communications for demand response and energy efficiency in commercial buildings," 2006.

[8] H. Hao, A. Kowli, Y. Lin, P. Barooah, and S. Meyn, "Ancillary service for the grid via control of commercial building HVAC systems," in *American Control Conf.*, 2013, accepted.

[9] NERC Resources Subcommittee, "Blancing and frequency control," North American Electric Reliability Corporation, Tech. Rep., 2011.

[10] B. Tashtoush, M. Molhim, and M. Al-Rousan, "Dynamic model of an HVAC system for control analysis," *Energy*, vol. 30, no. 10, pp. 1729–1745, 2005.

[11] W. Z. Huang, M. Zaheeruddin, and S. Cho, "Dynamic simulation of energy management control functions for HVAC systems in buildings," *Energy Conversion and Manage.*, vol. 47, pp. 926–943, 2006.

[12] PJM, "PJM manual 12: Balancing operations, rev. 27," December 2012.

[13] Y. Lin, T. Middelkoop, and P. Barooah, "Issues in identification of control-oriented thermal models of zones in multi-zone buildings," in *Conf. on Decision and Control,*. IEEE, 2012, pp. 6932–6937.

[14] S. Goyal and P. Barooah, "A method for model-reduction of non-linear thermal dynamics of multi-zone buildings," *Energy and Buildings*, 2011.

[15] Y. Lin, S. Meyn, and P. Barooah, "Commercial building HVAC system in power grid ancillary services," http://plaza.ufl.edu/yashenlin, University of Florida, Tech. Rep., 2013.

[16] American Society of Heating, Refrigerating and Air Conditioning Engineers, "The ASHRAE handbook fundamentals (SI Edition)," 2005.

[17] S. Goyal, H. Ingley, and P. Barooah, "Occupancy-based zone climate control for energy efficient buildings: Complexity vs. performance," *Applied Energy*, vol. 106, pp. 209–221, June 2013.

[18] X. Zhou and J. E. Braun, "A simplified dynamic model for chilled-water cooling and dehumidifying coils Part 1: Development (RP-1194)," *HVAC&R Research*, vol. 13, no. 5, pp. 785–804, 2007.

[19] Y. Yao, Z. Lian, and Z. Hou, "Thermal analysis of cooling coils based on a dynamic model," *Applied thermal engineering*, vol. 24, no. 7, pp. 1037–1050, 2004.

[20] A. Elmahdy and G. Mitalas, "A simple model for cooling and dehumidifying coils for use in calculating energy requirements for buildings," *ASHRAE transactions*, vol. 83, no. 2, pp. 103–117, 1977.

[21] B. A. Ogunnaike and W. H. Ray, *Process dynamics, modeling, and control*. Oxford University Press New York, 1994.

[22] I. B. Rhodes, "A tutorial introduction to estimation and filtering," *IEEE Transaction on Automatic Control*, vol. AC-16, no. 6, 1971.

[23] Daikin Industries, "Daikin McQuay Tools Suite," http://www.daikinmcquay.com/McQuay/DesignSolutions/McQuayToolsEngineers.

[24] Federal Energy Regulatory Commission, "Order No.755 Frequency Regulation Compensation in the Wholesale Power Markets: Comments of ISO/RTO Council," May 2011.

[25] J. Eyer and G. Corey, "Energy storage for the electricity grid: Benefits and market potential assessment guide," *Sandia National Laboratories Report, SAND2010-0815, Albuquerque, New Mexico*, 2010.